Dalton Transactions

Accepted Manuscript

ROYAL SOCIETY OF CHEMISTRY

www.rsc.org/dalton

Journal Name

RSCPublishing

ARTICLE

Oxygen nonstoichiometry, defect structure and oxygen diffusion in the double perovskite $GdBaCo_2O_{6-\delta}$

Cite this: DOI: 10.1039/xoxxoooooox

Received ooth January 2012,
Accepted ooth January 2012

DOI: 10.1039/xoxxoooooox

www.rsc.org/

D.S. Tsvetkov*[a], M.V. Ananjev[a,b], V.A. Eremin[b], A.Yu.Zuev[a] and E.Kh. Kurumchin[b]

Oxygen nonstoichiometry of $GdBaCo_2O_{6-\delta}$ was studied by means of thermogravimetric technique in the temperature range 600-1000 °C. The defect structure model based on simple cubic perovskite $GdCoO_{3-\delta}$ was shown to be valid for $GdBaCo_2O_{6-\delta}$ up to temperature as low as 600 °C. Two independent methods such as dc-polarization with YSZ microelectrode and ^{18}O-isotope exchange with gas phase analysis were used to determine oxygen self-diffusion coefficient in the double perovskite $GdBaCo_2O_{6-\delta}$. All measurements were carried out using ceramic samples identically prepared from the same single phase powder of $GdBaCo_2O_{6-\delta}$. The experimental data on oxygen nonstoichiometry of $GdBaCo_2O_{6-\delta}$ allowed precise calculation of the oxygen interphase exchange rate and the oxygen tracer diffusion coefficient on the basis of the isotope exchange measurements. The values of oxygen self-diffusion coefficient measured by dc-polarization technique were found to be in very good agreement with ones of the oxygen tracer diffusion coefficient.

Introduction

Complex oxides with the double layered perovskite-type structure such as $GdBaCo_2O_{6-\delta}$ have already received great attention in past decade [1-10] as promising cathode materials for intermediate temperature solid oxide fuel cells (IT–SOFCs) [1, 2]. Taskin et al. [3] were the first who showed that ordering of RE (rare-earth) and Ba cations in the A-sublattice of $REBaB_2O_{6-\delta}$ (B=Co; Mn) can significantly promote oxygen diffusion. They found fast oxygen diffusion in $GdBaCo_2O_{6-\delta}$ at temperatures as low as 400 °C. Chemical diffusion coefficient and surface exchange coefficient for $GdBaCo_2O_{6-\delta}$ were calculated as a function of temperature (T) at oxygen partial pressure (pO_2) of 1 bar from the results of transient TG (thermogravimetric) measurements [3]. Later Tarancon et al. [4] measured oxygen self-diffusion coefficient in $GdBaCo_2O_{6-\delta}$ as a function of T in the range between 299 and 686 °C at pO_2=0.2 bar using ^{18}O – isotope exchange depth profiling (IEDP) coupled with secondary ion mass spectrometry (SIMS). Recent measurements were performed by Song et al. [5] by means of conductivity relaxation technique. Oxide ion conductivity of the double perovskites $REBaCo_2O_{6-\delta}$ was calculated by Zhang et al. [6] on the basis of the oxygen permeability measured by them. For the sake of comparison the values of chemical diffusion coefficient reported by Taskin [3] and Song [5] can be recalculated into tracer diffusion one using the well-known expressions

$$\tilde{D}_O = D_O \cdot \theta \qquad (1)$$

and

$$\theta = \frac{1}{2}\frac{\partial \ln p_{O_2}}{\partial \ln c_O} = \frac{c_O}{2}\frac{\partial \ln p_{O_2}}{\partial c_O} = -\frac{6-\delta}{2}\frac{\partial \ln p_{O_2}}{\partial \delta}, \qquad (2)$$

where $\tilde{D}_O$, D_O, θ, c_O, $6-\delta$ and δ – are oxygen chemical diffusion coefficient, oxygen tracer diffusion coefficient, thermodynamic enhancement factor, concentration of oxygen ions in oxide lattice, oxygen content in the oxide per formula unit and oxygen nonstoichiometry of the oxide, respectively. Thermodynamic enhancement factor was calculated on the basis of pO_2 –T –δ diagram of $GdBaCo_2O_{6-\delta}$ which will be presented further (see Figs. 3 and 4). Oxide ion conductivity estimated by Zhang et al. [6] can be also recalculated into oxygen self-diffusion coefficient using the following equations

$$\sigma_{O^{2-}} = 2FU_{O^{2-}}c_O = \frac{(2F)^2}{RT}D_O c_O = \frac{(2F)^2}{RT}D_O\frac{(6-\delta)\cdot a}{N_A V_C}, \qquad (3)$$

$$D_O = \frac{\sigma_{O^{2-}} RTN_A V_C}{(2F)^2 a(6-\delta)}, \qquad (4)$$

where $\sigma_{O^{2-}}$, R, N_A, V_C, F, a – are oxide ion conductivity, universal gas constant, Avogadro constant, unit cell volume, Faraday constant and number of formula units of $GdBaCo_2O_{6-\delta}$ per unit cell, respectively.

All results mentioned above [3-6] along with those simulated using molecular dynamics method (MD) by Parfitt et al. [8] and Hermet et al. [9, 10] are shown in Fig. 1. As seen in Fig. 1 a discrepancy between the values of oxygen self-diffusion coefficient in $GdBaCo_2O_{6-\delta}$ determined by different authors reaches two orders of magnitude. Generally speaking a significant scattering in the data is a distinctive feature of

diffusion measurements (see, for example, Ref. [11]). The origin of the aforementioned discrepancy is of key importance. In this respect it is of great interest to understand either a difference in the experimental techniques applied or, oppositely, one in the real composition of a sample employed for the measurements mostly contribute in such discrepancy.
Oxygen nonstoichiometry of $GdBaCo_2O_{6-\delta}$ was measured early by us [7] within relatively high temperature range between 900 and 1050 °C whereas it is of great interest to provide such measurements at lower temperatures since this double perovskite is regarded as a very promising material for intermediate temperatures applications.

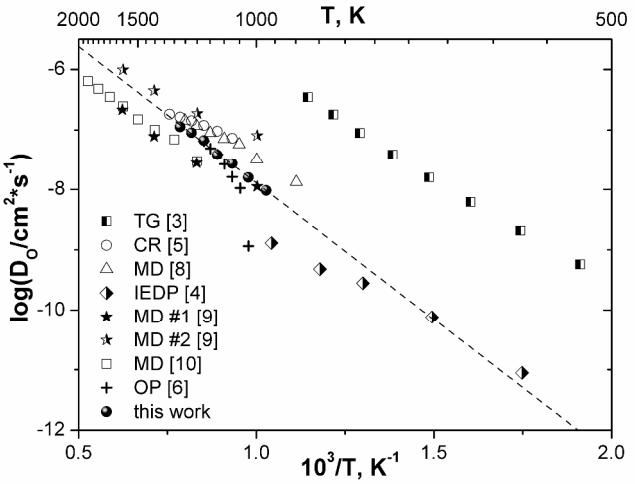

Fig. 1. Oxygen self-diffusion coefficient vs. *T* determined by different methods in air: TG – thermogravimetry; CR – conductivity relaxation; MD – molecular dynamics; OP – oxygen permeation. Dashed line extrapolates results of the present work to high and low temperatures.

Therefore, the priority purposes of the present work were (i) to measure oxygen nonstoichiometry of $GdBaCo_2O_{6-\delta}$ in the temperature range between 600 and 1000 °C by means of TG, (ii) to determine oxygen diffusion coefficient in $GdBaCo_2O_{6-\delta}$ using the identically prepared samples by means of two different methods such as polarization technique with $Zr_{0.9}Y_{0.1}O_2$ microelectrode and ^{18}O – isotope exchange with gas phase analysis, and (iii) to compare the results obtained accordingly with each other and with literature ones.

Experimental

Powder sample of double perovskite $GdBaCo_2O_{6-\delta}$ was prepared by means of glycerol – nitrate method using Gd_2O_3, $BaCO_3$, Co as starting materials. All materials used had a purity of 99.99 %.
Stoichiometric mixture of the starting materials was dissolved in concentrated nitric acid (99.99% purity) and required volume of glycerol (99% purity) was added as a complexing agent and a fuel. Glycerol quantity was calculated according to full reduction of corresponding nitrates to molecular nitrogen N_2. As prepared solution was heated continuously at 100 °C till complete water evaporation and pyrolysis of the dried precursor. The resultant ash was subsequently calcined at 1100 °C for 10 hours in air for formation of the double perovskite powder. Afterwards the latter was cooled slowly to room temperature.

The phase composition of the $GdBaCo_2O_{6-\delta}$ powder sample prepared accordingly was studied at room temperature by means of X-ray diffraction (XRD) with a DRON-6 diffractometer using Cu K_α radiation. XRD pattern of as-prepared single phase powder sample of the nominal composition $GdBaCo_2O_{5.515}$ is given in Fig. 2. The XRD pattern was indexed using the orthorhombic Pmmm space group with cell parameters ***a***=3.873(1) Å, b=7.815(8) Å, ***c***=7.530(7) Å which are quite consistent with those reported for $GdBaCo_2O_{6-\delta}$ earlier [3,4,6]. The results of the structureless Le Bail fitting (χ^2=2.082) are also shown in Fig. 2.

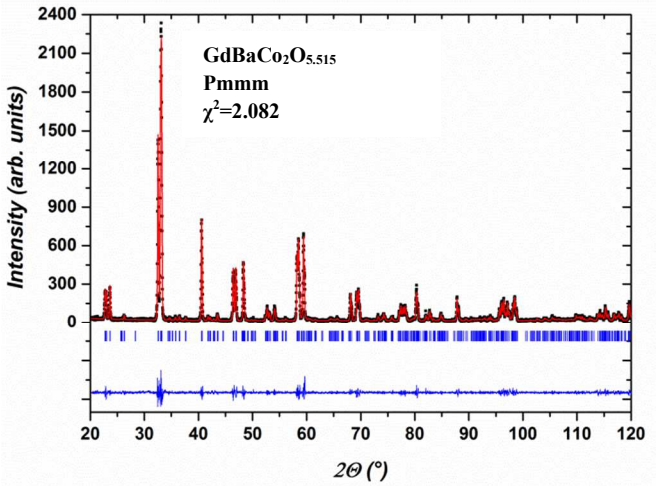

Fig. 2. Pattern matching refinement plot of $GdBaCo_2O_{5.515}$: observed X-ray diffraction intensity (■) and calculated curve (red line). The bottom blue curve is the difference of patterns, $y_{obs}-y_{cal}$, and the small blue bars indicate the angular positions of the allowed Bragg reflections.

The stoichiometric chemical composition of the $GdBaCo_2O_{6-\delta}$ single phase powder was confirmed by both the ICP technique using a spectrometer ICAP 6500 DUO (Thermo Scientific, USA) and the atomic absorption one using a spectrometer Solaar M6 (Thermo Scientific, USA) within the accuracy of 2%.
The single phase powder of $GdBaCo_2O_{6-\delta}$ was pressed into tablets of 9 mm in diameter and 2-3 mm in thickness and sintered at 1200 °C for 24 hours in air. Relative density of ceramic samples prepared accordingly was 95%. These ceramic tablets were polished to 0.8-1.0 mm thickness and used for the polarization and the ^{18}O isotope – exchange measurements.
Oxygen nonstoichiometry of $GdBaCo_2O_{6-\delta}$ as a function of *T* and pO_2 was studied by means of the thermogravimetric technique using a STA409PC TG setup (Netzsch, Germany). This technique is described in detail elsewhere [12]. Absolute value of oxygen nonstoichiometry in the $GdBaCo_2O_{6-\delta}$ samples was determined by two independent methods such as direct reduction of the oxide sample by hydrogen flux directly in TG setup (TG/H_2) and iodometric titration of the oxide sample preliminary annealed at 1000 °C for two hours in air and then slowly cooled (~100 °C/hour) to room temperature. Both methods are described in detail elsewhere [7, 12].
Oxide ion conductivity in $GdBaCo_2O_{6-\delta}$ was measured as a function of *T* and pO_2 by means of the polarization technique with a glass encapsulated YSZ microelectrode. This technique was described earlier in detail by Wiemhoefer et al. [13].
Oxygen exchange kinetics was studied using isotope exchange method with gas phase analysis using the original static circulation setup shown in Fig. 3 [14].

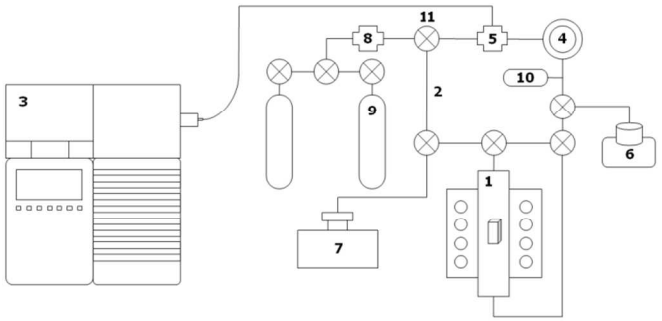

Fig. 3. Setup for ^{18}O-isotope exchange with gas phase analysis. 1 – reactor with $GdBaCo_2O_{6-\delta}$ sample; 2 – gas circuit; 3 – Agilent 5973N quadrupole mass spectrometer; 4 – circulation pump; 5 – dosing needle valve; 6 – rotary-vane rough pump; 7 – magnetic discharge diode pump; 8 – automatic inlet system; 9 – gas cylinders; 10 –total pressure transducer; 11 – vacuum valves.

The setup consists of the reactor (1) containing the $GdBaCo_2O_{6-\delta}$ specimen and a gas circuit (2). Isotope composition of the gas phase is monitored by an Agilent 5973N quadrupole mass spectrometer (*3*). Total volume of the gas circuit with the reactor is equal to 500 ml. This setup allows monitoring the oxygen isotope composition of the gas phase *in situ* during exchange experiment. To prevent probable gas diffusion limitations circulation pump (*4*) is used.

Isotope exchange experiment included the following steps:

1) *Ad initium* the whole system was evacuated to the residual pressure about 10^{-11} atm.
2) The setup was filled with the oxygen of natural isotope composition up to the desired pressure.
3) Reactor (1) with the sample was heated up to the measurement temperature. $GdBaCo_2O_{6-\delta}$ sample was equilibrated at given temperature and oxygen pressure for about 12 hours.
4) Reactor (1) was closed after the sample equilibration. Oxygen was pumped out from the rest of the gas circuit (except reactor) to the residual pressure about 10^{-11} atm.
5) Gas circuit was then filled with oxygen enriched with ^{18}O isotope up to the same total pressure. The circulation pump (4) was switched-on and the reactor (1) with the $GdBaCo_2O_{6-\delta}$ sample was opened.
6) The change of concentration of all oxygen species ($^{16}O_2$, $^{16}O^{18}O$, and $^{18}O_2$) in the gas atmosphere caused by redistribution of different oxygen isotopes between one and the sample were monitored using mass spectrometer (*3*).

Steps 2–6 were repeated at different temperatures and oxygen pressures.

Oxygen diffusion coefficient and surface exchange rate of the double perovskite $GdBaCo_2O_{6-\delta}$ were calculated from the experimental data $C_i=f(t)$, where t is time and i denotes i-oxygen species ($^{16}O_2$, $^{16}O^{18}O$, and $^{18}O_2$ molecules), on the basis of the Klier and Kucera exchange kinetics model [15]. According to this model isotope diffusion in a solid phase which is in dynamic equilibrium with gas phase can be described, omitting the isotope effect, by the Fick's second law

$$\frac{\partial \alpha}{\partial \tau} = D\nabla^2\alpha\,, \qquad (5)$$

where α, D and τ are the fraction of ^{18}O isotope in the gas phase, the oxygen diffusion coefficient in the bulk of solids and time, respectively. The fraction of ^{18}O isotope in the gas phase can be calculated according to the following equation

$$\alpha = \frac{n_{18}}{n_{18}+n_{16}} = \frac{1}{2}C_{34} + C_{36}\,, \qquad (6)$$

where n_{18}, n_{16}, C_{32}, C_{34}, C_{36} – are numbers of ^{18}O and ^{16}O atoms and fractions of $^{16}O_2$, $^{16}O^{18}O$ and $^{18}O_2$ molecules in a gas phase, respectively.

The number of adsorbed oxygen atoms is assumed [15] to be negligible as compared to the number of lattice oxygen atoms or those on the oxide surface. All oxygen atoms on the oxide surface are equivalent, i.e. the surface is uniform. The shape of a solid sample can be considered as a plate. In this case, the following boundary conditions can be written

$$-N_S\frac{\partial \alpha_S}{\partial \tau} = H\cdot S(\alpha-\alpha_S) - \frac{N_V\cdot D}{L}\left(\frac{\partial \alpha}{\partial r}\right)\Bigg|_{r=L} \qquad (7)$$

and

$$\left(\frac{\partial \alpha}{\partial r}\right)\Bigg|_{r=0} = 0\,, \qquad (8)$$

where H is the interphase exchange rate, i.e. the number of oxygen atoms exchanging on the unit surface area per unit time, N_S and N_V are the number of oxygen atoms on the surface and in the volume of the oxide sample, respectively, α_S and S are the ^{18}O isotope fraction on the sample surface and sample surface area, L is a half thickness of the sample, r is a coordinate of diffusion.

Numbers of oxygen atoms N_S and N_V on the surface and in the volume of the oxide sample were calculated as follows

$$N_S = \frac{V_S}{V}N_0 = \frac{S_m\cdot m\cdot r_O}{m/\rho}N_0 = \rho S_m r_O N_0 \qquad (9)$$

and

$$N_V = N_0 - N_S\,, \qquad (10)$$

where V_S, V, S_m, m, ρ, r_O and N_0 are volume of surface layer, total volume of the oxide sample, its specific surface area, mass, density, ionic radius of oxygen and total number of oxygen atoms in the oxide sample, respectively. It is worth noting that N_0 value was calculated using the data on oxygen nonstoichiometry of $GdBaCo_2O_{6-\delta}$ obtained in the present work.

The set of initial conditions can be given as follows

$$\begin{cases}\alpha = \alpha^0\\ \alpha_S = \alpha_S^0\end{cases} \text{ at } \tau = 0\,. \qquad (11)$$

Solution of the Fick's equation derived by Klier and Kucera [15] with respect to the initial and boundary conditions gives the expression describing a time dependence of ^{18}O oxygen isotope fraction in the gas phase

$$\alpha(\tau) = \gamma_0 + (\alpha^0 - \alpha_S^0)\sum_{n=1}^{\infty} B_n^{-1}\cdot\exp\left(\frac{D\beta_n^2}{L^2}\tau\right), \qquad (12)$$

where

$$B_n = \frac{1}{2}\left(1+\frac{N_S}{N_g}+\frac{N_V}{N_g}\right)+ \\ +\beta_n^2\left[\begin{array}{l}\dfrac{\left(N_g/2\right)+N_S+\left(N_S^2/2N_g\right)}{N_V}+\\ +\dfrac{D}{HSL^2}\left(\dfrac{N_g}{2}-N_S+N_V\right)\end{array}\right]+ \\ +\beta_n^4\left[\left(N_S+N_V\right)\frac{N_g D^2}{2(HS)^2L^4}-\left(N_S+N_g\right)\frac{N_S D}{N_V HSL^2}\right]+ \\ +\beta_n^6\left[\frac{N_g N_S^2 D^2}{2N_V(HS)^2L^4}\right] \qquad (13)$$

and N_g is a number of oxygen atoms in the gas phase.

Terms β_n in Eq. (11) are the roots of the following transcendental equation

$$\frac{\beta\left(1+\left(N_S/N_g\right)-\beta^2\left(N_S D/HSL^2\right)\right)}{\left(N_V/N_g\right)-\beta^2\left(N_V D/HSL^2\right)} = -tg\beta \qquad (14)$$

Eq. (12) along with Eqs. (13) and (14) was employed as a fitting equation for the experimental data analysis using original software written in Borland Delphi 7.0. The fitted parameters, therefore, were interphase exchange rate, *H*, and oxygen tracer diffusion coefficient, *D*.

Results and discussion

Oxygen nonstoichiometry and defect structure

The oxygen nonstoichiometry of the double perovskite $GdBaCo_2O_{6-\delta}$ measured by means of TG (this work) and coulometric technique (CT) [7] as a function of oxygen partial pressure and temperature in the ranges $-6 \le \log(p_{O2}/\text{atm}) \le -0.68$ and $650 \le T$, °C ≤ 1050, respectively, is given in Fig. 4 in comparison with the data early reported by Taskin et al. [3].

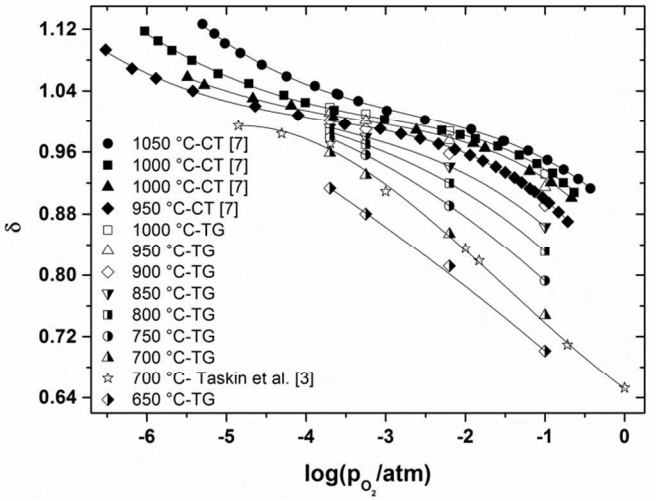

Fig. 4. Oxygen nonstoichiometry of $GdBaCo_2O_{6-\delta}$ vs. p_{O2} at different temperatures. Symbols represent the experimental data; lines – guide to eye.

As seen there is good agreement between the values on oxygen nonstoichiometry obtained by us and those measured by Taskin et al. [3]. It also follows from Fig. 4 that oxygen nonstoichiometry determined earlier by us [7] using the coulometric titration technique and one measured by the TG method in the present work are completely coincident with each other.

The modeling of the defect structure of the double perovskite $GdBaCo_2O_{6-\delta}$ was carried out by considering different reference states in our previous paper. Only the model based on the cubic perovskite $GdCoO_3$ as a reference state was shown [7] to fit the experimental data on oxygen nonstoichiometry of $GdBaCo_2O_{6-\delta}$ really good. Within the framework of this model oxygen vacancies ordering can be described by formation of the electrostatic cluster $(V_O^{\bullet\bullet} - Ba'_{Ba})^{\bullet}$ according to the following reaction

$$V_O^{\bullet\bullet} + Ba'_{Gd} \Leftrightarrow (V_O^{\bullet\bullet} - Ba'_{Gd})^{\bullet}. \qquad (15)$$

The well known reaction of charge disproportionation involving the transfer of an electron between adjacent $Co_{Co}^{\times}$ sites

$$2Co_{Co}^{\times} = Co_{Co}^{/} + Co_{Co}^{\bullet} \qquad (16)$$

and one of the formation of oxygen vacancy during the process of oxygen release from the cobaltite lattice under reducing conditions

$$O_O^{\times} + 2Co_{Co}^{\bullet} = \frac{1}{2}O_2 + V_O^{\bullet\bullet} + 2Co_{Co}^{\times} \qquad (17)$$

have been taken into account as well [7].

The fitting function

$$\log(p_{O_2}/atm) = 2\log\left(\frac{2K_2^{-1}K_1(6-\delta)(A+1-2\delta)^2}{B(A+2\delta)^2}\right), \qquad (18)$$

where

$$A = \frac{(K_3-4)(2\delta-1)+\sqrt{4\delta K_3(K_3-4)(\delta+1)+K_3(K_3+12)}}{2(K_3-4)}, \qquad (19)$$

$$B = K_1(\delta-1)-1+\sqrt{K_1^2(\delta-1)^2+2K_1(\delta+1)+1}, \qquad (20)$$

K_1, K_2, and K_3 are the equilibrium constants of the reactions (15), (16), and (17), respectively, has been derived [7] for the defect structure of the double perovskite $GdBaCo_2O_{6-\delta}$. Since the oxygen nonstoichiometry was measured in relatively narrow temperature range the equilibrium constants in the fitting Eq. (18) were substituted by their temperature dependencies $K_i = K_i^0 exp(-\Delta H_i/RT)$, where ΔH_i is an enthalpy of appropriate defect reaction.

The model function Eq. (18) along with Eqs. (19) and (20) was used for verification of the defect structure model using the expanded experimental data on the oxygen nonstoichiometry of $GdBaCo_2O_{6-\delta}$. The results of such verification by least square method are shown in Fig. 5. As seen the model proposed fits the experimental data on oxygen nonstoichiometry of $GdBaCo_2O_{6-\delta}$ within the whole temperature range investigated in our previous work and present study. It allows to conclude that the defect structure model proposed [7] is valid for $GdBaCo_2O_{6-\delta}$ up to temperature as low as 650 °C. However, equilibrium constants obtained as functions of temperature as a result of defect structure model fitting to experimental data on oxygen nonstoichiometry allow calculation of oxygen content in $GdBaCo_2O_{6-\delta}$ at least up to temperature as low as 400 °C. Oxygen content in $GdBaCo_2O_{6-\delta}$ calculated at 400 °C on the basis of the fitting results was almost equal to that measured by Taskin et al. [3]. Therefore, the values of oxygen content in $GdBaCo_2O_{6-\delta}$ at 600 °C necessary for analysis of the results of

oxygen isotope exchange at this temperature were calculated using defect structure model.

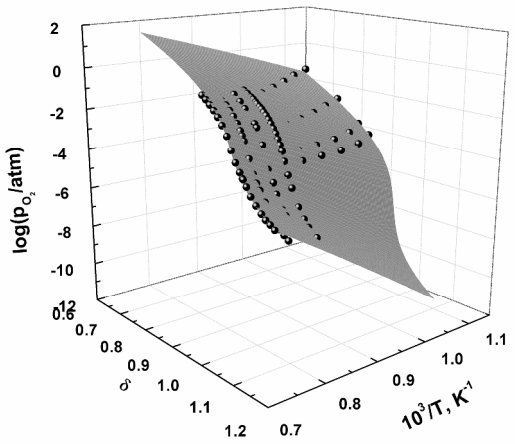

Fig. 5. Oxygen nonstoichiometry and nonlinear surface fitting results of the defect structure model for $GdBaCo_2O_{6-\delta}$. Points – experimental data, surfaces – fitted model [7].

Oxygen exchange and diffusion

Typical variation of concentration of different oxygen species ($^{18}O_2$, $^{16}O^{18}O$ and $^{16}O_2$) depending on time is shown in Fig. 6. These experimental data given in Fig. 6 were obtained at pO_2=1400 Pa and T=600 °C. The fraction, α, of ^{18}O isotope in the gas phase equilibrated with the oxide sample was calculated according to Eq. (6) and shown in Fig. 7 as a function of time at pO_2=1400 Pa and T=600 °C. The least square fitting results of the model Eq. (12) are shown in Fig. 7 as well. The interphase exchange rate, H, and oxygen tracer diffusion coefficient, D_O, determined accordingly are given in Fig. 8 as a function of pO_2 at different temperatures. As seen interphase exchange rate is proportional to $p_{O_2}^{n_H}$ with n_H slightly increasing from 0.7 at 600 °C to 0.85 at 850 °C.

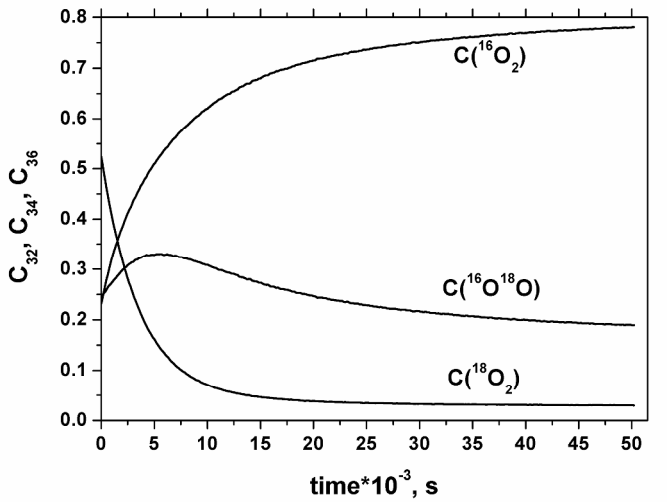

Fig. 6. Concentration of different oxygen molecules ($^{18}O_2$, $^{16}O^{18}O$ and $^{16}O_2$) vs. time in typical isotope exchange experiment at pO_2=1400 Pa and T=600 °C.

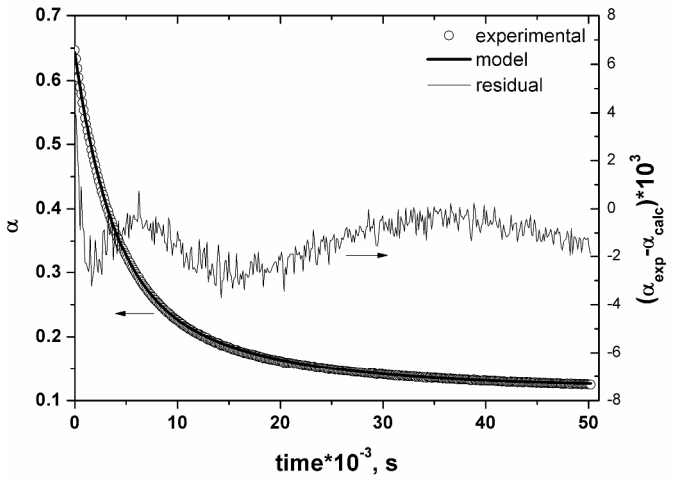

Fig. 7. Fraction of ^{18}O-isotope in gas phase vs. time in typical isotope exchange experiment at pO_2=1400 Pa and T=600 °C. Points – experimental data, line – fitting result using Eq. (12).

Surface exchange coefficient, k, of $GdBaCo_2O_{6-\delta}$ was calculated using relationship given by

$$k = H\frac{M_r}{(6-\delta)N_A\rho}, \qquad (21)$$

where M_r, N_A, ρ are sample molar weight, Avogadro constant and sample density respectively.

For the sake of comparison k as a function of temperature is shown in the inset of Fig. 8a along with the data available in literature. The analysis of the oxygen exchange will be given in detail in forthcoming publication.

According to Fig. 8b the oxygen tracer diffusion coefficient, in contrast to the interphase exchange rate, decreases with increasing pO_2 most likely due to simultaneous oxygen vacancies (as charge carriers) concentration decrease (see Fig. 4).

Oxide ion transport in $GdBaCo_2O_{6-\delta}$ was also independently studied in the present work by means of polarization technique [16]. Current–voltage (I–V) curves measured using YSZ glass encapsulated microelectrode in contact with $GdBaCo_2O_{6-\delta}$ sample are given in Fig. 9a. Oxide ion conductivity, σ_{ion}, of $GdBaCo_2O_{6-\delta}$ calculated from the slope coefficient of these I–V curves is shown in Fig. 9b as a function of pO_2 at different temperatures. As seen σ_{ion} is almost constant within the temperature range between 700 and 750 °C and one slightly grows with pO_2 decrease in temperature range between 800 and 850 °C. Such behavior is quite expected. Actually using obvious relation between diffusion coefficient of oxygen (D_O) and one of oxygen vacancy ($D_{V_O^{\bullet\bullet}}$)

$$D_{V_O^{\bullet\bullet}}\delta = D_O(6-\delta) \qquad (22)$$

Eq. (4) can be rewritten as

$$\sigma_{O^{2-}} = B\cdot D_{V_O^{\bullet\bullet}}\delta, \qquad (23)$$

where $B = \frac{(2F)^2}{RT}\cdot\frac{a}{N_A V_C}$.

As follows from Eq. (23) change of oxide ion conductivity with oxygen nonstoichiometry depends on slope coefficient, $B\cdot D_{V_O^{\bullet\bullet}}$, which increases with increasing temperature due to

simultaneous increase of oxygen diffusion coefficient as shown in Fig. 8b.

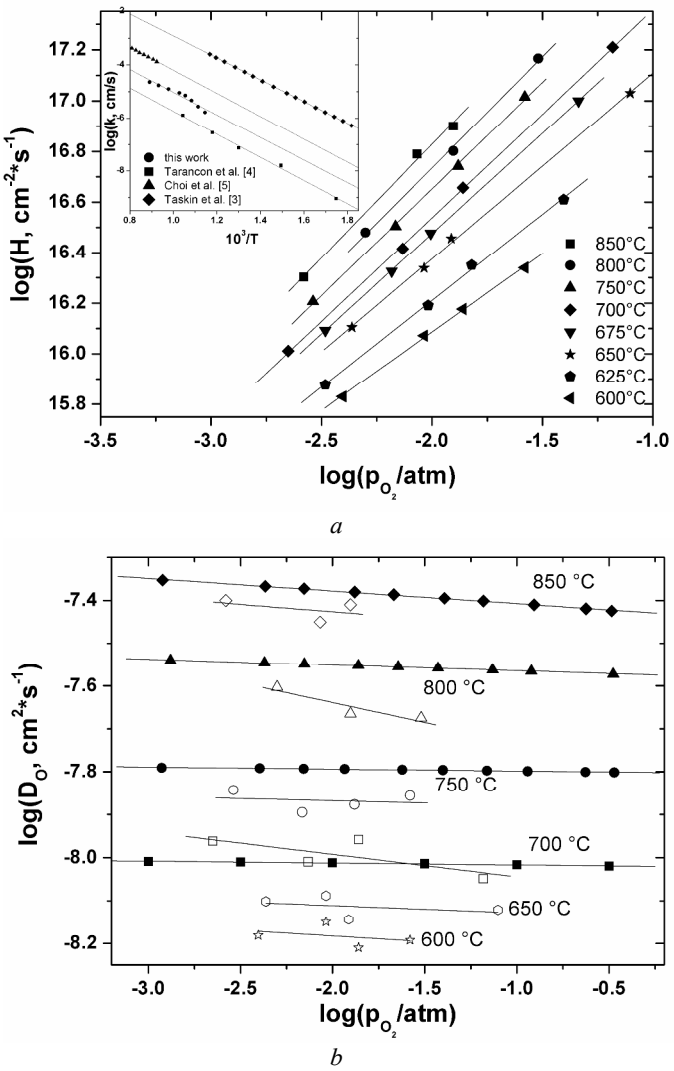

Fig. 8. Interphase exchange rate (*a)* and oxygen self-diffusion coefficient (*b)* vs. pO_2 at different temperatures. Open and closed symbols correspond to results of isotope exchange and dc-polarization, respectively.

Oxygen diffusion coefficient of $GdBaCo_2O_{6-\delta}$ calculated from σ_{ion} using Eq. (4) is shown in Fig. 8b in comparison with the tracer oxygen diffusion coefficient measured by isotope exchange technique. Really good agreement is obviously seen between two sets of oxygen diffusion coefficients. Such coincidence of the results obtained by means of completely different methods but using identically prepared samples may imply that aforementioned discrepancy in the data on oxygen diffusivity in $GdBaCo_2O_{6-\delta}$ (see Fig. 1) mostly caused by the differences in the microstructure or real composition of the samples used for measurements provided by different authors. Figure 1 shows that the values of oxygen diffusion coefficient in $GdBaCo_2O_{6-\delta}$ measured by us are in agreement only partly with those reported by different authors. Our data, for example, coincide with those reported by Zhang et al. [6] at temperatures higher than 777 °C, however, the latter do not exhibit any linear dependence. It is worth noting in this respect that only oxygen diffusion coefficients determined by us in present work as well as by Taskin et al. [3] and Hermet et al. [10] being plotted in logarithmic scale versus reciprocal temperature exhibit really linear behavior within the whole temperature range investigated as shown in Fig. 1. The temperature dependency of oxygen diffusion coefficient found in the present study and that plotted on the basis of MD simulation [10] have very similar slope coefficients (see Fig. 1) but the value of oxygen self-diffusion coefficient determined at a given temperature in this work exceeds that estimated in Ref. [10] on about half order of magnitude. Figure 1 also allows to regard the values of oxygen self-diffusion coefficient reported by Taskin et al. [3] as considerably overestimated as compared to those of other authors.

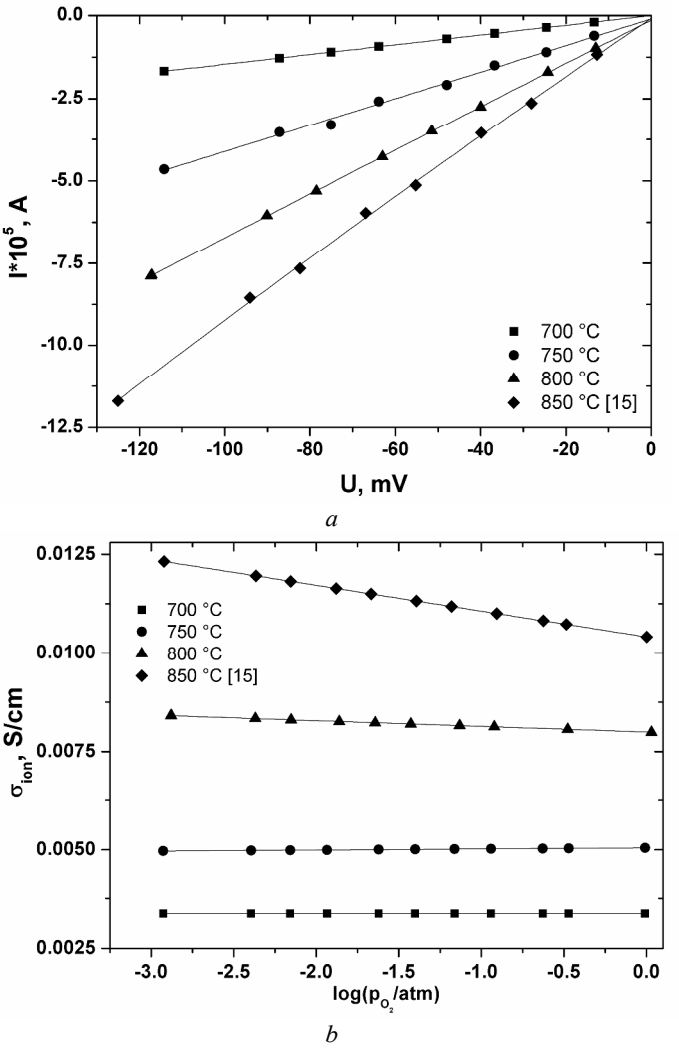

Fig. 9. Results of dc-polarization: current-voltage (*I-V*) curves measured using YSZ glass encapsulated microelectrode in contact with $GdBaCo_2O_{6-\delta}$ (*a*); oxide ion conductivity of $GdBaCo_2O_{6-\delta}$ vs. pO_2 (*b*) at different temperatures.

Conclusions

Oxygen nonstoichiometry of $GdBaCo_2O_{6-\delta}$ was studied depending on pO_2 at temperatures between 600 and 1000 °C by means of thermogravimetric technique. The modeling of the defect structure was carried out and the model based on simple

cubic perovskite $GdCoO_{3-\delta}$ as a reference crystal was shown to be valid for $GdBaCo_2O_{6-\delta}$ up to temperature as low as 600 °C. Oxygen self-diffusion coefficient in the double perovskite $GdBaCo_2O_{6-\delta}$ was measured by means of two independent methods such as dc-polarization with YSZ microelectrode and ^{18}O-isotope exchange with gas phase analysis. All diffusivity measurements were carried out using ceramic samples identically prepared from the same single phase powder of $GdBaCo_2O_{6-\delta}$. The obtained data on oxygen nonstoichiometry enabled precise calculation of the oxygen interphase exchange rate and the oxygen tracer diffusion coefficient on the basis of the oxygen isotope exchange measurements. The interphase exchange rate was found to be proportional to $pO_2^{n_H}$ with n_H slightly increasing with temperature. The oxygen tracer diffusion coefficient decrease observed with increasing pO_2 is caused most likely by simultaneous decrease of oxygen vacancies concentration in $GdBaCo_2O_{6-\delta}$. The values of oxygen self-diffusion coefficient measured by dc-polarization technique were found to coincide completely with those of oxygen tracer diffusion coefficient. Significant scattering in the literature data on oxygen diffusivity in the double perovskite $GdBaCo_2O_{6-\delta}$ was, therefore, assumed to be mostly caused by differences in the real composition and/or microstructure of the samples used by different authors. Interphase exchange rate was found to increase with increasing pO_2 due to simultaneous increase of the total number of exchanging atoms whereas oxygen self-diffusion coefficient decreases since oxygen vacancies concentration decreases at the same time.

Acknowledgements

This work is partly financially supported by the RFBR grant # 13-03-00519 and by the Federal Target Program # 2012-1.5-14-000-2019-002-8888.

Notes and references

[a] Department of Chemistry, Institute of Natural Sciences, Ural Federal University, Ekaterinburg, 620000, Russia, e-mail: dmitry.tsvetkov@urfu.ru.

[b] Institute of High Temperature Electrochemistry, Ural Division of Russian Academy of Sciences, Ekaterinburg, 620000, Russia.

1 A. Chang, S.J. Skinner , J.A. Kilner, *Solid State Ionics*, 2006, **177**, 2009

2. N. Li, Z. Lu, B. Wei, X. Huang, K. Chen, Y. Zhang, W. Su, *J. Alloy. Compd*., 2008, **454**, 274
3. A.A. Taskin, A.N. Lavrov, Y. Ando, *Appl. Phys. Lett.*, 2005, **86**, 091910
4. A. Tarancon, S.J. Skinner, R.J. Chater, F. Hernandez-Ramırez, J.A. Kilner, *J. Mater. Chem.*, 2007, **17**, 3175
5. M.-B. Choi, S.-Y. Jeon, J.-S. Lee, H.-J. Hwang, S.-J. Song, *J. Power Sources*, 2010, **195**, 1059
6. K. Zhang, L. Ge, R. Ran, Z. Shao, S. Liu, Acta Materialia 56 (2008) 4876
7. D.S. Tsvetkov, V.V. Sereda, A.Yu. Zuev, *Solid State Ionics*, 2010, **180**, 1620
8. D. Parfitt, A. Chroneos, A. Tarancon, J.A. Kilner, *J. Mater. Chem.*, 2011, **21**, 2183
9. J. Hermet, G. Geneste, G. Dezanneau, *Appl. Phys. Lett.*, 2010, **97**, 174102
10. J. Hermet, B. Dupé, G. Dezanneau, *Solid State Ionics*, 2012, **216**, 50
11. J.L. Routbort, R. Doshi, M. Krumpelt, *Solid State Ionics*, 1996, **90**, 21
12. D.S. Tsvetkov, I.L. Ivanov, A.Yu. Zuev, *Solid State Ionics*, 2012, **218**, 13
13. H.-D. Wiemhoefer, H.-G. Bremes, U. Nigge, W. Zipprich, *Solid State Ionics*, 2002, **150**, 63
14. M.V. Ananyev, E.Kh. Kurumchin, *Russ. J. Phys. Chem. A*, 2010, **84**, 1039
15. K. Klier, E. Kucera, *J. Physics Chem. Solids*, 1966, **27**, 1087
16. D.S. Tsvetkov, V.V. Sereda, A.Yu. Zuev, *Solid State Ionics*, 2011, **192**, 215

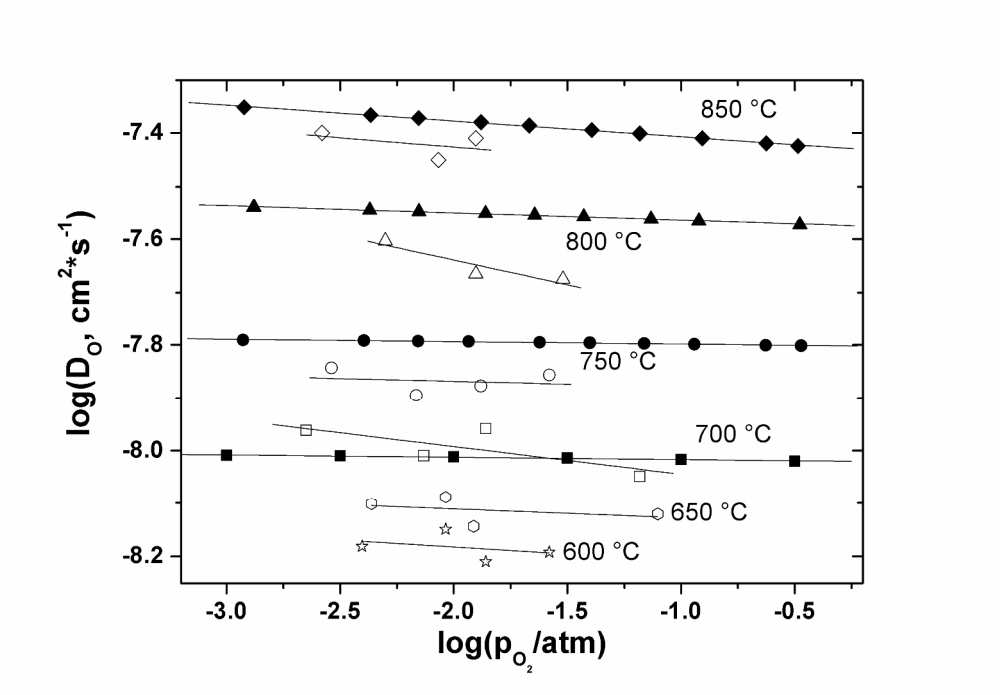

The values of oxygen self-diffusion coefficient measured by dc-polarization technique completely coincide with those of oxygen tracer diffusion coefficient.
289x203mm (300 x 300 DPI)